A Novel Metamaterial FSS-based Structure for Wideband Radome Applications

Shiv Narayan[1] and R M Jha[1]

Abstract A novel metamaterial based FSS (frequency selective surfaces) structure is presented in this paper for wideband airborne radome applications. The proposed metamaterial-FSS structure consists of three layers, where a DPS (double positive sign) layer is sandwiched between a MNG (μ-negative) and ENG (ε-negative) layer, exhibits very good bandpass characteristics inside the operational band along with excellent roll-off characteristics outside the band. The EM performance analysis of the proposed structure has been carried out using *transmission line transfer matrix* (TLTM) method, which shows excellent bandpass characteristics over wide frequency range. The transmission efficiency is over 95% both at normal incidence and at high incidence angles of 30°, and 60°. The frequency range extends from S- to X-band (2.5-9.9 GHz). In view of streamlined airborne radome applications, the reflection properties and *insertion phase delay* (IPD) are also determined at high incident angles.

Keywords: Metamaterial, Metamaterial-FSS, Transmission line transfer matrix method.

1 Introduction

The frequency selective surface (FSS) structures have been widely used as spatial filter in aerospace sector such as *radar absorbing structures* (RAS), radomes, dichroic plate, and dual band reflectors in the microwave and millimeter wave frequency regime. For radome applications, the filter response should fully transmit the signal inside the operational band and completely reject it outside the band of interest.

Such required radome band characteristics were realized by multilayered FSS structures using conventional FSS design (Munk, 2000). However this led to higher insertion loss at the bandpass and complexity of the fabrication process. In addition to this, the frequency response of conventionally designed FSS structure is affected by the mutual interactions between the resonant unit cells of the array. This necessitates a large FSS screen size, which causes limitations in application where incident EM wave does not have uniform phase front.

Recently, metamaterial have attracted many researchers due to its unusual electromagnetic properties (negative permittivity and permeability), resulting in design and development of various metamaterial based devices such as metamaterial-FSS radome (Narayan *et al*., 2012), metamaterial invisibility cloak (Choudhury *et al*., 2013), and metamaterial for wireless power transfer (Stevens, 2013). In order to enhance the performance of conventional FSS, numerous works have been presented to design the metamaterial based FSS filters (Sarabandi and Behdad, 2007; Sun *et al*., 2008; Chiu and Chang, 2009) for single as well as dual-band characteristics. However, these filters have narrow bandpass characteristics and also require better roll-off characteristics outside the band.

In view of possible applications, the EM performance analysis of tri-layer metamaterial-FSS structure is presented in this paper based on *transmission line transfer matrix* (TLTM) method. The proposed MTM-FSS structure exhibits excellent bandpass characteristics over a wide frequency range of 2.5-9.9 GHz. The objective of the present work is to design a metamaterial-FSS based radome wall configuration, which can provide superior bandpass response required for the streamlined airborne radome applications.

2 Theoretical Considerations

The EM performance analysis of tri-layer metamaterial FSS has been carried out in this work using *transmission line transfer matrix* (TLTM) method. The TLTM method is the combination of *transmission line method* (TLM) and *transfer matrix method* (TMM). This method is applicable for both TE and TM polarizations at both the normal and oblique angles of incidence. In TLTM method, a multilayered planar structure is represented by an equivalent transmission line. Each transmission line section is described by a characteristic impedance and propagation constant, which depends on the

[1] CSIR-National Aerospace Laboratories, Bangalore, 560017, India

incidence angle, frequency, and polarization of incident wave. The tangential components at the consecutive layers are related to each other, and the reflection and transmission coefficients of the total structure can be calculated for different polarizations. A side view of a tri-layer metamaterial FSS structure is shown in Figure 1.

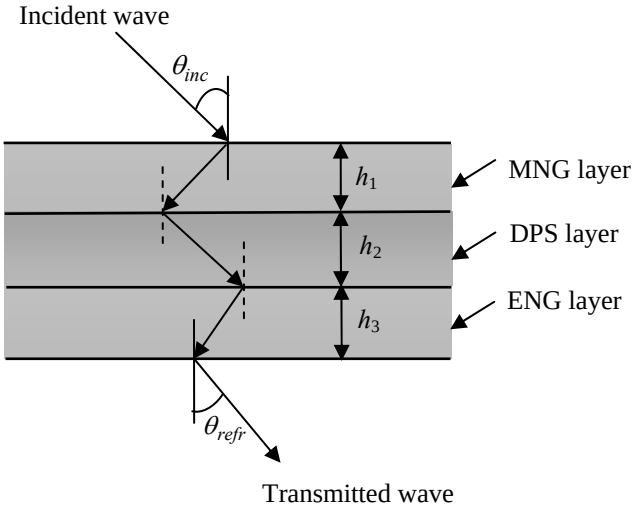

Figure 1: Side view of tri-layer metamaterial FSS structure.

By using Snell's law, the relationship between the two adjacent layers l^{th} and $(l+1)^{th}$ can be expressed as

$$\gamma_l \sin\theta_l = \gamma_{(l+1)} \sin\theta_{(l+1)} \tag{1}$$

where γ_l is the propagation constant and is given by

$$\gamma_{lz} = j\omega\sqrt{\mu_l \varepsilon_l}\cos\theta_l \tag{2}$$

where ε_l and μ_l are permittivity and permeability of the l^{th} layer, respectively. $\omega = 2\pi f$ is the angular frequency. θ_l denotes the incidence angle at the l^{th} layer. The characteristic impedances for both TE and TM waves can be expressed as

$$Z_{0l}^{TE} = \eta_l \sec\theta_l \tag{3}$$

$$Z_{0l}^{TM} = \eta_l \cos\theta_l \tag{4}$$

The transfer matrix of the whole structure can be determined by

$$[T]_{(l+1)l} = [L]_{(l+1)}[I]_{(l+1)l}, \quad l = 0,1, \ldots (N-1) \tag{5}$$

where N is the number of layers. The wave amplitude transmission matrix $[L]_{(l+1)}$ and discontinuity transmission matrix $[I]_{(l+1)}$ can be calculated using the expressions given in Oraizi and Afsahi (2009).

The transmission coefficient (t) and reflection coefficient (r) of the total structure can be expressed as

$$\begin{bmatrix} t \\ 0 \end{bmatrix} = [T]_{(N+1)0}\begin{bmatrix} 1 \\ r \end{bmatrix} \tag{6}$$

where

$$[T]_{(N+1)0} = [T]_{(N+1)N}[T]_{N(N-1)} \ldots\ldots [T]_{(l+1)l} \ldots\ldots [T]_{10} \tag{7}$$

The power reflection R, and power transmission T, of the proposed structure can be determined by

$$R = rr^* \tag{8}$$

$$T = tt^* \tag{9}$$

In the present work, the Drude dispersion models are used to compute the relative permittivity of the ENG structures (wire structure). By using the Drude's model, the complex relative permittivity are computed by Pendry *et al*. (1999)

$$\varepsilon_r = \varepsilon - \frac{\omega_{ep}^2}{(\omega^2 + j\Gamma_e)} \tag{10}$$

where ω_{ep} is the electric plasma frequency. Γ_e is the electric damping factor. ε represents the permittivity matrix of the medium. The electric plasma frequency can be given as

$$\omega_{ep} = \sqrt{\frac{2\pi c^2}{p^2 \ln\frac{p}{r}}} \tag{11}$$

where c is the speed of light. r and p represent the radius of wire and periodicity of the wire structure, respectively. The electric damping factor can be determined as

$$\Gamma_e = \frac{\varepsilon_0 \left(p\omega_{ep}\right)^2}{r^2 \pi\sigma} \tag{12}$$

where σ represents the conductivity of the metal.

According to the Lorentz and Resonance models (Pendry *et al*., 1996; Smith *et al*., 2000), the permeability at the microwave frequencies may be realized by a periodic array of resonators (SRR). The complex relative permeability of *circular split ring resonator* (CSRR) can be given by

$$\mu_{eff} = 1 - \frac{\left(f_{mp}^2 - f_{m0}^2\right)}{f^2 - f_{m0} - j\Gamma_m f} \qquad (13)$$

where f_{mo} and f_{mp} are the magnetic resonant frequency and magnetic plasma frequency of the SRR, respectively. Γ_m represents the magnetic damping factor.

The *insertion phase delay* (IPD) is defined as the delay that occurs for an electromagnetic wave *w.r.t.* the free-space transmission, when it passes through the radome wall. The insertion phase delay is a measure of phase distortion through the radome wall, which is expressed by Kozakoff (1997)

$$IPD = -\left(\angle T_1 + \angle T_2 + \angle T_3 + \ldots \angle T_n\right) - 2\pi \sum_{i=1}^{n} \frac{d_i}{\lambda_i} \cos\theta_i \qquad (14)$$

where d_i and λ_i are the thickness and the wavelength of wave in each layer respectively. $\angle T_i$ represents the phase angle associated to the power transmission coefficient. θ_i denotes the angle of incidence at each layer.

3 EM Design Aspects of Tri-layer Metamaterial FSS

In this work, the proposed metamaterial-FSS structure consists of three layers as shown in Figure 2, where a DPS (double positive sign) layer is sandwiched between a MNG (μ-negative) and ENG (ε-negative) layers. In the EM design, Foam (relative permittivity, ε_r =1.15, and electric loss tangent, $\tan\delta_e = 0.0018$) is considered as a dielectric medium of DPS layer. The MNG layer is composed of *circular split ring resonators* with dielectric medium of Polyethylene (ε_r = 3.66 and $\tan\delta_e = 0.0014$), and its relative permeability is computed by the relation (13).

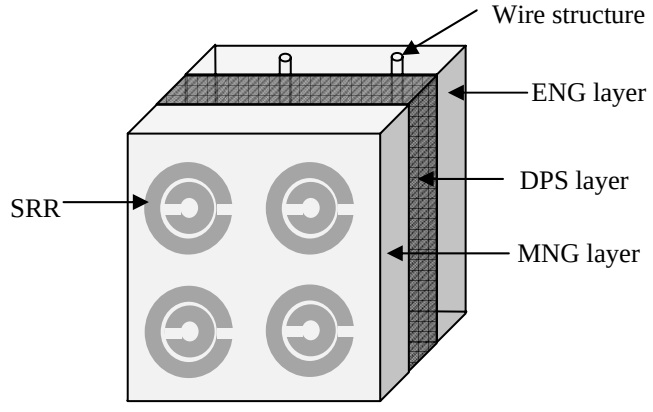

Figure 2: Schematic of a tri-layer metamaterial structure.

The complex relative permeability *vs*. frequency for different value of separation between the rings is shown in Figure 3. The design dimensions of the split ring resonator are optimized as periodicity, p = 8 mm, radius of the ring, a = 3.2 mm, separation between the rings, d = 0.02 mm, and thickness of the ring, w = 0.30 mm. The ENG layer consists of wire structure with μ_r = 1 and dielectric medium of Teflon (ε_r =2.0 and $\tan\delta_e = 0.0003$). The relative permittivity of the wire structure is computed by the equation (10). The complex relative permittivity versus frequency of the wire structure of ENG layer is presented in Figure 4. The optimized dimensions of the wire structure are periodicity, p = 6 mm and radius of the wire, r = 10 μm.

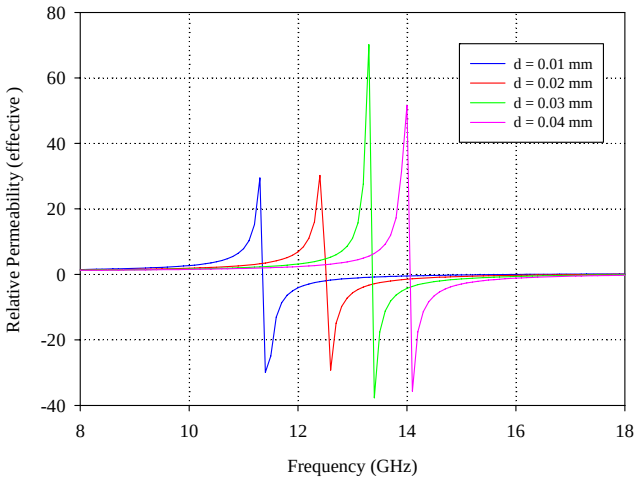

Figure 3: Relative permeability (effective) *vs*. frequency of SRR of MNG layer for different separations (d) between the rings of the SRR.

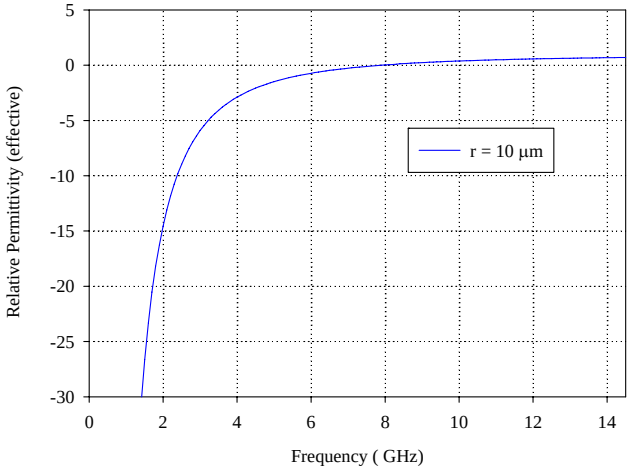

Figure 4: Relative permittivity (effective) *vs*. frequency of wire structure of ENG layer.

The thicknesses of the proposed metamaterial-FSS layers is optimized to be 1.0 mm for MNG layer, 2.4 mm for DPS layer, and 1.0 mm for ENG layer. The electric plasma frequency of the wire structure is determined by using the relation (11). Here the wire structure is designed for the plasma frequency, f_{ep} = 7.886 GHz and electric damping factor, Γ_e = 42.95 MHz. The split ring resonator is designed for the magnetic resonant frequency, f_{om} = 12.55 GHz, magnetic plasma frequency, f_{mp} = 17.75 GHz, and magnetic damping factor, Γ_m = 0.299

4 EM Performance Analysis

Since in practice, the evaluation of EM performance of a radome for perpendicular polarization (TE polarization) is very critical. The EM performance analysis of tri-layer metamaterial-FSS have been investigated in this paper for TE polarization based on TLTM method. In order to show the superiority of proposed metamaterial-FSS based radome over the conventional radome, a monolithic radome is designed using quartz dielectric material (ε_r =3.12 and $\tan\delta_e = 0.011$), with the wall thickness as that of total thickness of proposed metamaterial-FSS radome (4.4 mm).

The transmission and reflection characteristics of this monolithic radome are analyzed at normal incidence, 30°, and 60° for TE polarization as shown in Figures 5 and 6. Further, the transmission and reflection characteristics of the proposed metamaterial-FSS are studied at normal as well as high incident angles such as 30°, and 60° for TE polarization as shown in Figures 5 and 6. It is observed that the transmission efficiency of the monolithic radome is good (> 90%) up to 2.3 GHz at normal incidence and beyond this frequency, it is degraded to 60-70%. Moreover, the transmission efficiency of monolithic radome is degraded more rapidly *w.r.t.* the frequency at higher incidence angles. While the proposed metamaterial-FSS radome exhibits more than 95% transmission efficiency over a wide frequency ranges from S- to X-band (2.5-9.9 GHz). In addition, the bandpass characteristic of metamaterial-FSS radome is independent of incident angles, which is a unique feature of the metamaterial based structure.

Moreover, the power reflection is also very low (< 4%) over the frequency range from 2.5-9.9 GHz at normal incidence, 30°, and 60° as shown in Figure 6. Whereas the power reflection of monolithic radome is very high (up to 35% at normal incidence) over the frequency of interest and it is further increases with the angle of incidence as shown in Figure 6. Thus the proposed metamaterial-FSS based structure for radome application shows excellent transmission efficiency (> 95%) and very low reflection (< 4%) as compared to the conventional monolithic radome over the frequency of interest.

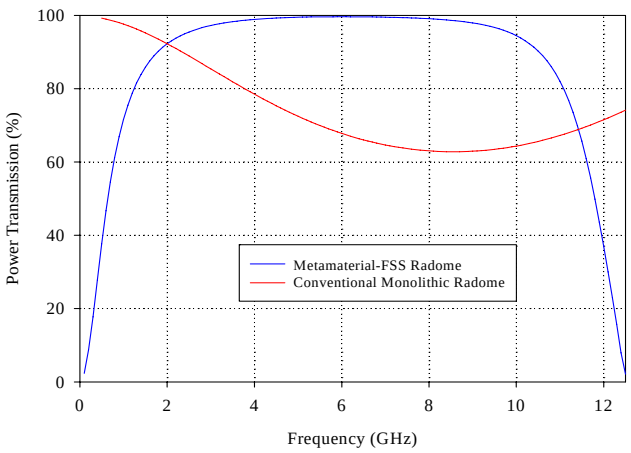

(a)

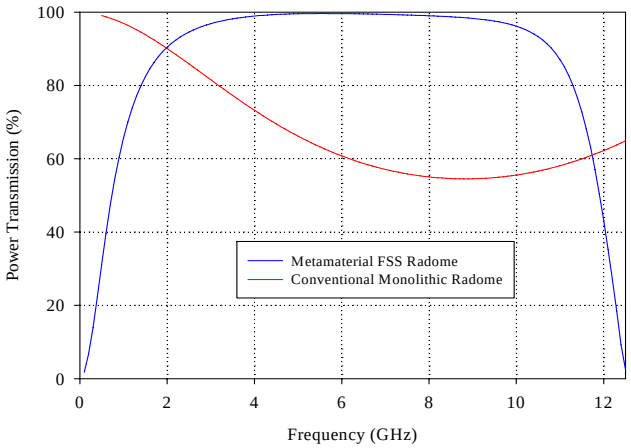

(b)

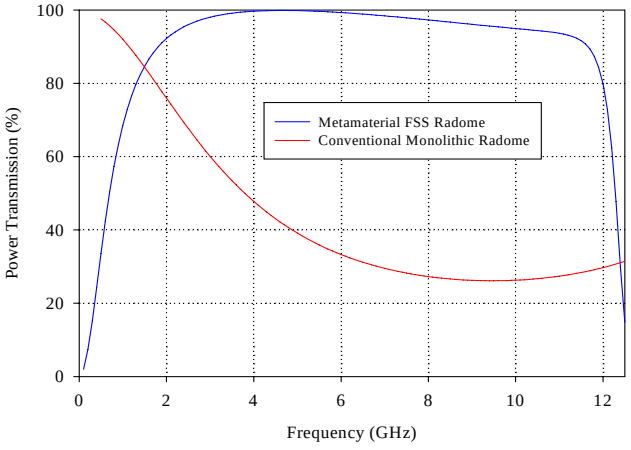

(c)

Figure 5: Power transmission characteristics of tri-layer metamaterial-FSS for TE polarization at incidence angles: (a) 0°, (b) 30°, and (c) 60°.

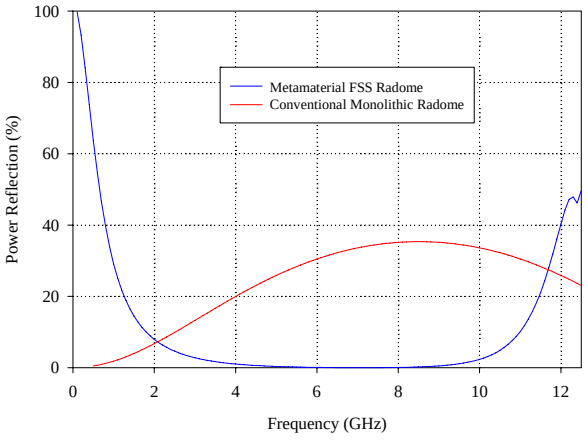

(a)

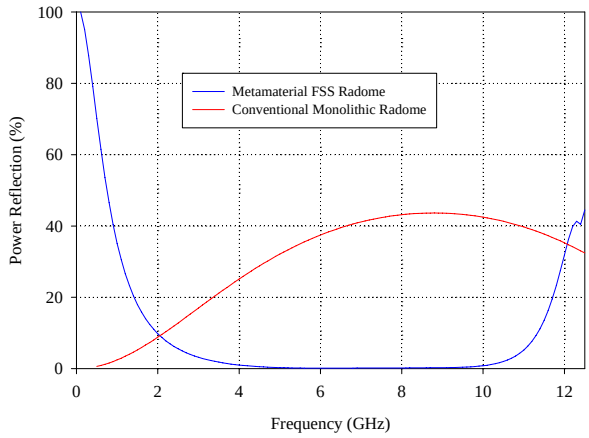

(b)

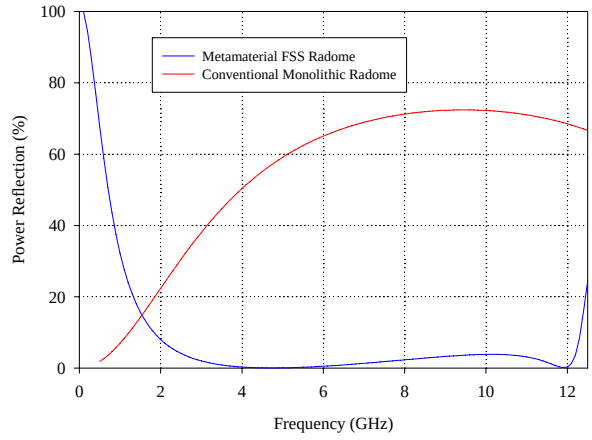

(c)

Figure 6: Power reflection characteristics of tri-layer metamaterial-FSS for TE polarization at incidence angles: (a) 0°, (b) 30°, and (c) 60°.

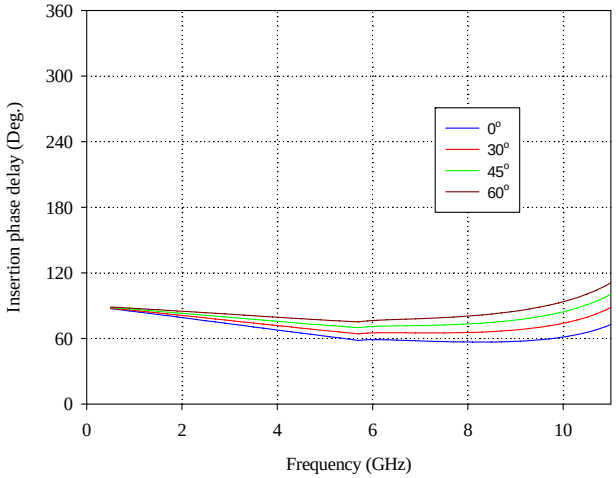

Figure 7: Insertion phase delay characteristics of tri-layer metamaterial FSS for TE polarization at incidence angles 0°, 30°, 45°, and 60°.

Further, the insertion phase delay (IPD) of the proposed metamaterial-FSS structure is computed using equation (14). In view of streamlined radome applications, IPD is analyzed at normal as well as high incident angles (30°, 45°, and 60°) for perpendicular polarization as shown in Figure 7. It is observed that the IPD of the tri-layer metamaterial-FSS does not show rapid variation *w.r.t.* the operating frequency (Fig. 7), which is desirable for radome applications. Thus the proposed metamaterial-FSS structure as whole can be used potentially as the radome wall.

5 Conclusions

The EM performance analysis of metamaterial based FSS structure has been studied in the present paper using TLTM method. It is found that the proposed metamaterial based FSS structure showed superior EM performance as compared to the conventional monolithic radome. The proposed structure exhibited more than 95% power transmission over a wide frequency range from S- to X-band (2.5-9.9 GHz) at normal incidence as well as at high incident angles, and showed excellent roll-off characteristics outside the band. In addition, the proposed structure showed very low reflection (< 4%) over the frequency of interest. The superior EM performance of the proposed tri-layer metamaterial-FSS configuration makes it suitable for the design of normal incidence as well as streamlined broadband airborne radomes.

References:

Chiu, C.; Chang K. (2009): A novel miniaturized-element frequency selective surface having a stable resonance. *IEEE Antennas and Wireless Propagation Letter*, vol. 8, pp. 1175-1177.

Choudhury, B.; Jha, R.M. (2013): A review of metamaterial invisibility cloaks. *Computers, Materials & Continua*. (In press)

Kozakoff, D.J. (1997): *Analysis of Radome-Enclosed Antenna*. Artech House, Boston.

Munk, B.A. (2000): *Frequency Selective Surfaces: Theory and Design.* John Wiley, New York

Narayan, S.; Shamala, J.B.; Nair, R.U.; Jha, R.M. (2012): Electromagnetic performance analysis of novel multiband metamaterial FSS for millimeter wave radome applications. *Computers, Materials & Continua,* vol. 31, no. 1, pp. 1-16.

Oraizi, H.; Afsahi M. (2009): Design of metamaterial multilayer structures as frequency selective surfaces. *Progress In Electromagnetics Research C,* vol. 6, pp. 115-126.

Pendry, J.B.; Holden, A.J.; Robbins, D.J.; Stewart, W.J. (1999): Magnetism from conductors, and enhanced non-linear phenomena. *IEEE Transactions on Microwave Theory and Techniques*, vol. 47, pp. 2075-2084.

Pendry, J.B.; Holden, A.J.; Stewart, W.J.; Youngs, I. (1996): Extremely low frequency plasmons in metallic mesostructures. *Phys. Rev. Lett.,* vol. 76, pp. 4773-4776

Sarabandi, K.; Behdad, N. (2007): A frequency seletive surface with minitiatirized elements. *IEEE Transactions on Antennas and Propagation*, vol. 55, pp. 1239-1245.

Smith, D.R.; Padilla, W.J.; Vier, D.C.; Nemat-Nasser, S.C.; Schultz, S. (2000): Composite medium with simultaneously negative permeability and permittivity. *Phy. Rev. Lett.,* vol. 84, pp. 4184-4187.

Stevens, C.J. (2013): Power transfer via metamaterials. *Computers, Materials & Continua*, vol. 33, no. 1, pp. 1-18.

Sun, Q.H.; Cheng, Q.; Xu, H.S.; Zhou, B.; Cui, T.J. (2008): A new type of band-pass FSS based on metamaterial structures. 2008 *International Workshop on Metamaterials*, Nanjing, China, pp. 267-269.